Accessing Icy World Oceans using Lattice Confinement Fusion Fast Fission

Theresa L. Benyo, Ph.D. (NIAC Fellow, NASA GRC), Lawrence P. Forsley (Co-PI, NASA GRC/GEC), Rodger Dyson, Ph. D. (NASA GRC, Power Conversion), Michael Becks (NASA GRC /HX5, MCNP Modeling)

Introduction

NASA's Ocean Worlds Exploration Program [1,2] has the challenge of penetrating the many kilometer-thick ice caps in its search for extraterrestrial life on icy worlds. These icy ocean worlds include Ceres, Europa, Enceladus, and Pluto. Each world may have a liquid water ocean beneath their ice crust. These oceans are likely heated by the parent planet's tidal forces, or in the case of Pluto or Ceres, by residual radioactive decay. A robotic probe exploring the oceans beneath must either melt or bore through the ice crust first. Consequently, the proposed probe needs to contend with hydrostatic ice pressure, ice phase and density changes, then water pressure. Such a mission requires a small, but robust and long lived, electrical energy and heat source.

Figure 1. Artistic rendering of a robotic probe capable of melting through icy shelves of planets, moons, or asteroids.

The proposed innovation is a compact, scalable nuclear energy source that does not use highly enriched uranium (HEU), high-assay enriched uranium (HALEU), low enriched uranium (LEU) nor plutonium-238 (^{238}Pu). The nuclear energy source consists of a hybrid fusion-fast-fission method whereby neutrons generated from Lattice Confinement Fusion (LCF) are used to fission materials such as depleted uranium or thorium. LCF has been demonstrated by both NASA (published in Physical Review C [3]) and by Lawrence Berkeley National Laboratory (published in the Journal of Applied Physics [4]), and commercialized by Astral System, Ltd. [5] Although these methods are reminiscent of Low Energy Nuclear Reactions (LENR), both methods operate at much higher energies than any attempt at cold fusion. This new hybrid energy source is sufficient to provide power and heat for melting or boring through icy caps with untethered, autonomous probes. These probes can be used for planetary (i.e., Pluto), lunar (i.e., Enceladus), or asteroid (i.e., Ceres) exploration where icy caps are encountered. An example of one of these proposed robotic probes is shown in Figure 1.

As an alternative to only melting, we propose (ultra) sonically assisted ice fracturing, borrowing from Navy research on super-cavitating torpedoes while noting the Europa Tunnelbot [6] (as shown in Fig 2) proposed a sonar transceiver for navigation. Although high speed transit isn't expected (mission specifications expect 3 years to transit the ice [6]), super-cavitation involves a sheath of bubbles along a torpedo [7] thereby reducing friction with water. We recognize that the extreme pressures preclude bubble formation, but a thin skin of liquid water would be expected to form along the probe surface. This method is analogous to a possible means of penetrating ice via a melted ice sheath vibrating against and fracturing local ice. In addition, like sonar, a sonic transducer can operate in a pump-probe manner, listening to return echoes to measure ice density directly and possibly communicate to the surface from some depth within the ice.

During Phase I, the team developed models for a hybrid fusion fast fission sub-critical energy source, an energy conversion system, and a passive heat transfer system that can enhance the existing NASA Glenn Research Center (GRC) NASA Innovative Advanced Concepts (NIAC) Tunnelbot [6] and Jet

Figure 2. Conceptual illustration showing the Europa Tunnelbot traveling through the ice to the water underneath.

Propulsion Laboratory's (JPL) Cryobot [8] robotic probe designs. The hybrid fusion fission energy source is an alternative to ^{238}Pu heat sources and conventional fission reactors using enriched uranium products; low-enriched uranium (LEU) highly assayed low-enriched uranium (HALEU), or highly enriched uranium (HEU). The hybrid fusion fission energy source uses neutrons from Lattice Confinement Fusion (LCF) reactions to fission depleted uranium or thorium. Our modeling indicates this hybrid energy source with 12 kW_{th} total power is sufficient to provide power and heat for melting and drilling through icy caps with untethered, autonomous probes, however further work needs to be completed to improve the specific power of the LCF Fast Fission System (0.20 kW_{th}/kg). However, with 20% thermal to electric efficiency, 10 times more electrical power will be available for the LCF Fast Fission Reactor (4.2 kW_e) as compared to the Kilopower Reactor (420 W_e). Despite the larger reactor core mass, the LCF Fast Fission Reactor would require less shielding than for Kilopower as determined by the neutron flux determination by our calculations. In addition, the acoustic Stirling engine achieves high energy conversion efficiency (20% as mentioned above) and contains minimal moving parts to reduce mechanical failures. Rejected waste heat is transported via oscillating heat pipes as shown in Fig 3 for external ice phase management. The probe may also take advantage of the water skin layer on the vehicle's outer heated walls combining ice melting with ultrasonic drilling/cutting through the thick icy layer.

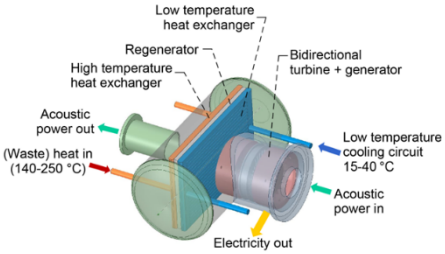

Figure 3. Oscillating heat pipes transport thermal energy from/to the acoustic Stirling heat exchangers.

Lattice Confinement Fusion Fast Fission

Deuterium (D or ^{2}H) is an isotope of hydrogen carrying with it a neutron. Deuterium-Deuterium (DD) fusion has conventionally required either large magnetic fields to hold an under-dense plasma (10^{14} ions/cm^3) or large lasers to briefly (1 nanosecond) compress a dense plasma (10^{26} ions/cm^3) [9]. Instead, Lattice Confinement Fusion (LCF) uses deuterated metals at high density (10^{23} ions/cm^3) where the deuterium is held indefinitely in a metal lattice [10, 11]. Conditions sufficient for fusion are created in the confines of the metal lattice that is held at ambient temperature. While the metal lattice, loaded with deuterium fuel, may initially be at room temperature, LCF creates an energetic environment inside the lattice where individual atoms achieve equivalent fusion-level kinetic energies. A key feature of LCF is the critical role played by metal lattice electrons whose negative charges help "screen" the positively charged deuterons. Such electron screening [11] allows adjacent fuel nuclei to approach one another more closely reducing the Coulomb barrier, thus reducing the chance they simply scatter off one another, and increases the likelihood that they tunnel through the electrostatic barrier promoting D-d fusion as shown in Fig 4.

LCF can be triggered and controlled by bremsstrahlung gamma beams or phonon-nuclear coupling resulting in an equivalent local deuteron ion temperature of up to 3 keV [12] kinetic energy as compared to the sun at 1.5 keV (17 million °C). Other triggers may be used to facilitate LCF such as electron beams,

x-ray beams, electrical current, and plasma glow discharge. Although a keV glow discharge provides insight into electron screening, the co-deposition process using electrical current as the trigger applies far more current, and hence electrons, at < 10 V [13]. In addition, LCF relies upon the electric and magnetic forces inherent in a metal lattice to constrain a low temperature plasma while the same electrons screen and either enhance the fusion rate or promote interactions with the metal lattice via Oppenheimer-Phillips [14] stripping reactions where energetic neutrons are captured by atoms in the metal lattice. These stripping reactions provide additional energetic particles such as energetic protons (~6 MeV). In addition, with enough electron screening, protons could be captured by atoms in the metal lattice and produce energetic neutrons (~6 MeV).

With all three ingredients, deuterium loaded in a metal lattice, electron screening and a trigger such as an electric current, energetic deuterons (d) impact and fuse with adjacent deuterons (D), resulting in standard products. The standard products are neutrons (n), helium-3/helion (^{3}He), protons (p), and tritium (t, T or ^{3}H). Two relatively equal probable outcomes are:

D+d → n (2.45 MeV) + ^{3}He (1 MeV)
D+d → p (3.02 MeV) + T (1 MeV)

Subsequently, the products shown above could then be part of further interactions producing helium-4 (^{4}He) such as:

D+T → n (14.1 MeV) + ^{4}He (3.5 MeV)
D+^{3}He → p (15.0 MeV) + ^{4}He (3.6 MeV)
T+T → 2n (1 to 9 MeV) + ^{4}He
^{3}He +^{3}He → 2p (1 to 10 MeV) + ^{4}He

Having neutrons produced via LCF with enough energy (>2MeV) to fission non-fissile materials such as thorium and natural uranium, an increasing amount of energy can be produced with a hybrid reactor. Here, hybrid fusion-fast fission takes advantage of both types of reactions where fusion reactions produce energetic neutrons up to 14.1 MeV that would be available to fission non-fissile materials. In fact, the method of lattice confinement fusion-fast fission of uranium has been demonstrated [15] through electrolytic wet cell experiments. These experiments apply a very low current to the wet cell system and co-deposits palladium (Pd) from a solution containing palladium chloride (PdCl), lithium chloride (LiCl) and

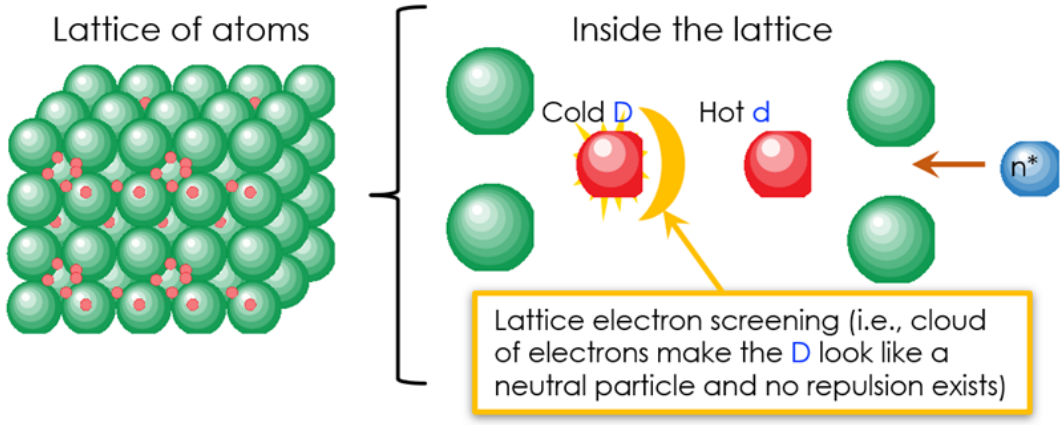

Figure 4. Diagram depicting Lattice Confinement Fusion assuming some sort of applied trigger (i.e. gamma beam) resulting in energetic neutrons being produced. The energetic neutrons impart kinetic energy to deuterons and with the help of electron screening produce d-D fusion.

heavy water (D_2O) onto a wire cathode. This combination creates a Pd metal lattice loaded with deuterium, and with enough electron screening, achieves LCF.

Lattice Confinement Fusion Fast Fission Mechanisms

The use of Pd to build the deuterated metal lattice on the composite (Pd, Cl and Li) cathode greatly increases the dissociation, adsorption and absorption of hydrogen isotopes known as spillover. Previously, an unoptimized natural uranium (U) [15] composite palladium/gold/lithium/uranium (Pd/Au/Li/U) cathode produced 10^4 to 10^6 neutrons/second until the system was arbitrarily shutdown after 33 hours. The neutrons produced averaged 6.4 MeV and were a combination of:

1. Fusion (2.45 and 14.1 MeV) neutrons,
2. Fission neutrons (peak at 1 MeV, average 2 MeV with a Maxwellian tail to 10+ MeV),
3. Stripping neutrons (averaging 6+ MeV).

However, the bulk of the neutrons appeared to be produced by deuteron proton capture via a stripping reaction on Pd. Pd isotopes have an average mass of 106 atomic mass unit (AMU) and a binding energy of 8.6 MeV/nucleon. The deuteron has a binding energy of 2.2 MeV. To successfully strip a proton or neutron from the deuteron onto a Pd atom requires "borrowing" binding energy from the Pd. The remaining energy, 8.6 – 2.2 MeV or 6.4 MeV appears as kinetic energy amongst the escaping neutron and the Pd nucleus. That energy is shared inversely proportionally to the mass of the Pd target and the neutron:

- Ratio of a neutron to the number of nucleons in Pd is 1:106 (^{106}Pd vs 1 p or n) = 0.0094.
- Portion of kinetic energy (KE) going to Pd is 0.0094 x 6.4 MeV = 0.0604 MeV, or 60 keV.
- Portion of the KE going to the neutron is 6.40MeV – 0.0604 MeV = 6.34 MeV.

In addition to 6+ MeV neutrons, the screened fusion fast proton fission of uranium or thorium also occurs. High purity germanium (HPGe) gamma detector data indicates that some of the uranium fission products were due to charged particle interactions in addition to fission.

The LCF D-d 2.5 MeV fusion neutrons have also been used to fast-fission natural thorium (^{232}Th) and uranium (both natural abundance and depleted uranium, DU) [15-17]. This hybrid method has been proposed to drive a deep space fission power system [16]. The non-optimized LCF fast fission power density is 1/3 that of the HEU-based Kilopower system [18] without using fissile isotopes. Recent work with the Naval Surface Warfare Centers (NSWC) has observed 90-200 watts-thermal/gram [19], without actinides, using a patented protocol [20]. This power output exceeds the ^{238}Pu 0.54 watt-thermal/gram in powering radioisotope thermal generators (RTGs).

LCF has also been carried out in a molten eutectic, lithium-deuterided salt at 500 °C [21]. Extending this fusion fast fission process to either thorium or depleted uranium should provide sufficient thermal energy to melt cryogenic ice while efficiently converting thermal to electric energy to power systems. In addition, this system would be able to change power output and ice melting rates rapidly that accommodates encountering the anticipated high-pressure ice phases and possible icy world sub-surface brine lakes much like the icy environments predicted on Enceladus.

Robotic Probe Design Comparison

Two robotic probe designs were studied by the team: the Europa Tunnelbot [6] and the JPL Cryobot [7, 22, 23]. Each probe design has aspects which together could determine a robotic probe sufficient for a mission to an icy world powered by a hybrid fusion fast-fission reactor.

A conceptual illustration of the Europa Tunnelbot design from Ref 6 is shown in Fig 2. The basis of this design is to use the heat generated from the power reactor to melt the ice around the robot. The Europa Tunnelbot uses either an RTG or a fission-based reactor based on the Kilopower design. The layout of the Europa Tunnelbot with the Kilopower reactor is shown in Fig 5 from Ref 6. The overall length of the Europa Tunnelbot is 5.3m with the reactor located well away (about 2.65m) from the sensitive electronics located in the robot. This placement along with a water shield in the void ensures that radioactive by-products from the nuclear reactor do not damage the other components in the robotic probe. Fig 6 from Ref 6 shows the Europa Tunnelbot based on the RTG heat source design. This robotic probe design is 5.7m long with RTG stacks along with most of the science instruments and all the electronics for the various other systems contained within the pressure vessel shown on the right side of Fig 6. The remaining parts: three repeaters, fiber optic cable spools, anchor cable spools, an antenna, and temperature and pressure sensors of this RTG-based design are contained within the unpressurized section of the robotic probe as shown in the left side of Fig 6. While the RTG-based design

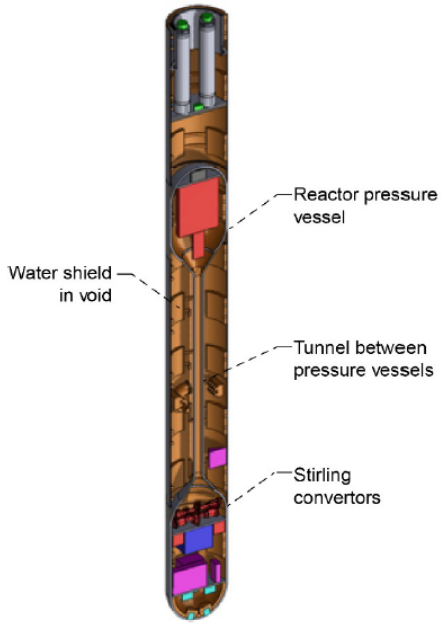

Figure 5. Cutaway showing placement of the power reactor in relation to other components of the Europa Tunnelbot.

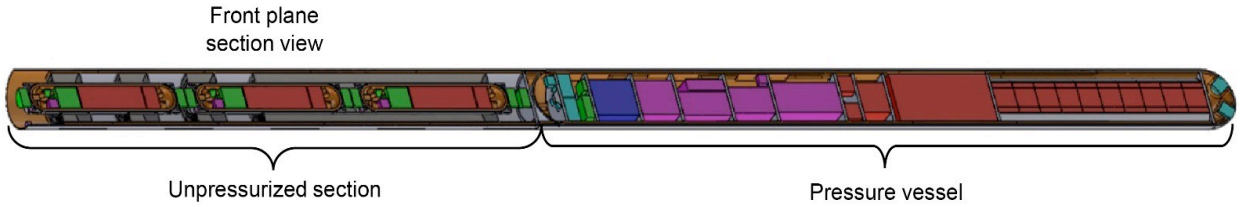

Figure 6. Cutaway showing placement of RTG heat source (shown in red on the far right) versus the science instruments and electronics shown in the pressure vessel. The unpressurized section contains three repeaters, fiber optic cable spools, anchor cable spools, an antenna, and temperature and pressure sensors.

allows for a smaller robotic probe, the available power (50 W_e) for the probe is much less than the Kilopower-based probe (400 W_e).

Similarly, the JPL Cryobot uses an RTG-based design for heat and power generation. Figure 7 from Ref 22 shows an illustration of the robotic probe with the components shown in the cutaway. The overall length of the JPL Cryobot is 3.9m long and 23cm in diameter. Here, the power system offers 1kWe (peak)

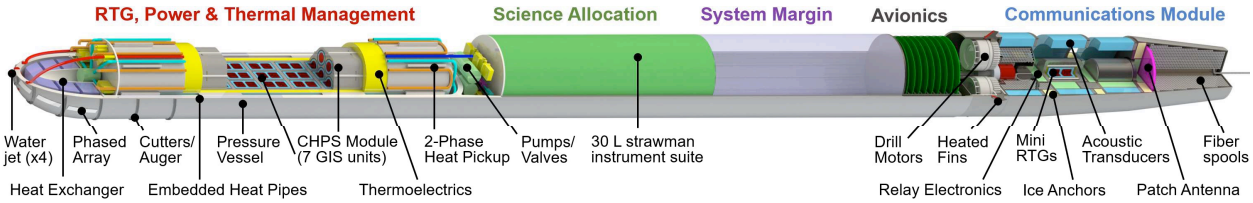

Figure 7. Conceptual model cutaway of JPL's Cryobot showing all the components of the RTG-based robotic probe.

and 10.5 kWt. The RTG system for this Cryobot design [24, 25] consists of 12 compact heat source modules (CPHS). Each CPHS contains seven ^{238}Pu graphite impact shell (GIS) modules. These modules can be seen in the left part of Fig 7. While the Cryobot design uses RTG for heat and power, the design also offers a water jet, an auger for drilling, and heated fins that are desirable for this current study. These features are not included in the Europa Tunnelbot design. The Cryobot's rear electrically heated fins could "cut" through the ice and provide drag stabilization, counter-torque for the drill, and differential drag for steering.

In both probe designs, there exist mechanical turbo pumps used for heat transfer. These types of pumps are difficult to maintain remotely. Another more passive device is desired. An Acoustic Stirling Quad Engine system [26] combined with oscillating heat pipes would be able to meet the need for no hot moving parts electricity generation and no pumped fluid heat transfer.

Table 1 shows the characteristics of each robotic probe as known from each team's studies. Our team envisions that the robotic probe designed as part of this study will be a hybrid of the 3 compared in the table. The hybrid design would consist of a Kilopower-type LCF fast-fission core as modified from the Europa Tunnelbot design, the Acoustic Stirling Quad Engine for heat transfer and electricity generation, the water jet, auger, and heated fins from the JPL Cryobot design, and all the necessary infrastructure and science instruments needed to complete an Icy Worlds Ocean mission.

Table 1. Comparison of Europa Tunnelbot vs JPL's Cryobot

	Europa Tunnelbot	Europa Tunnelbot	JPL Cryobot
Power/Heat Source	Kilopower	RTG	RTG
Electric Power	420 W_e	110 W_e	295 W_e
Thermal Power	43.3 kW_{th}	12 kW_{th}	10.5 kW_{th}
Landed Mass	1,350 kg	750 kg	350 kg
Robot Size	5.3 m long, 52 cm diam	5.7 m long, 25 cm diam	3.9 m long, 23 cm diam
Robot Volume	1,107 L	271 L	150 L
Total Power Density	0.04W/cc	0.04W/cc	0.07W/cc
Reactor Core/RTG Mass	44.4 kg	49 kg	57 kg
Reactor Core/RTG Size	25 cm long, 13 cm diam	59 cm long, 23 cm diam	1.1 m long, 18 cm diam
Reactor Core/RTG Volume	4.4 L or 4,417.9 cm^3	24.5 L or 24,513.1 cm^3	28.5 L or 28,500 cm^3
Reactor Total Power Density	9.9 W/cc	0.5 W/cc	0.4 W/cc
Reactor Specific Power	9.46 W_e/kg 0.97 kW_{th}/kg	2.24 W_e/kg 0.24 kW_{th}/kg	5.18 W_e/kg 0.18 kW_{th}/kg
Descent Rate (100K)	~50 cm/hr	~13 cm/hr	~25 cm/hr
Descent Rate (250K)	~85 cm/hr	~22 cm/hr	~180 cm/hr
Boring Mechanism	Melting tube	Melting tube	Water jet, drill, heated fins
Lifetime	~3 years	~10 years	2-6 years

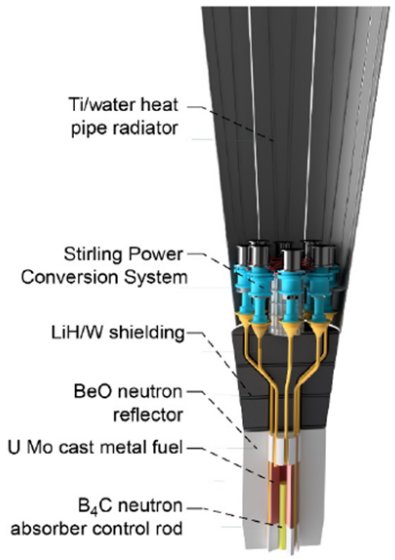

Figure 8. Kilopower (1 kW_e) reactor design

Robotic Probe Fusion Fission Power System

Like the Kilopower system of the Europa Tunnelbot, the proposed LCF fast-fission reactor should provide enough heat from the nuclear reactions it produces to power and heat the robotic probe. Considering the LCF fast-fission concept, the Europa Tunnelbot's Kilopower design (Fig 8 from Ref [6]) lends itself to easily modifying the core of the Kilopower reactor to a hybrid fusion-fission design. The advantage of LCF fast fission is that it requires less shielding based on the use of non-fissile materials. Neutrons produced by the fusion reactions would be consumed by the non-fissile material. MCNP models of Kilopower were used to modify the reactor core. Figure 9 from Ref 6 shows the MCNP geometry of the Kilopower model.

The advantage of the hybrid fusion fast-fission reactor is that it will not need fissile materials and as much shielding as the Tunnelbot. The design constraints and specifications of the hybrid reactor are shown in Table 2 and compared with the Kilopower design.

Table 2. Comparison of Kilopower fission-based reactor vs LCF hybrid fusion fission reactor.

	Kilopower System	LCF Fast Fission System
Nuclear Fuel	93% enriched solid cast ^{235}U Mo alloy	Deuterated natural uranium
Reactor	Fast spectrum, Be reflector, single centered control rod	Hybrid fusion fission
Heat Transport	1,100 K passive Na Heat Pipes	Oscillating Heat Pipes
Power Conversion	Stirling Convertors scaled from ASRG[a]	Acoustic Stirling Quad Engine
Design Life	>10 years	>10 years
Load Bus	120 Vdc	120 Vdc
Mass of the Reactor	44.4 kg	59.2 kg
Electric Power	420 W_e	4.2 kW_e
Thermal Power	43.3 kW_{th}	12 kW_{th}
Specific Power	0.97 kW_{th}/kg	0.20 kW_{th}/kg

[a]Advanced Stirling Radioisotope Generator

Although LCF can efficiently fast-fission depleted uranium and thorium [15-16, 27], this type of fission hasn't been done in a high-temperature, lithium-based molten salt. The MCNP modeling can reveal reactor material options allowing an appropriate hybrid fusion fast-fission nuclear reactor design. In addition to materials, the modeling can indicate alternative means of triggering LCF, effective high temperature operation and appropriate power conversion systems [26, 28]. For example, conducting LCF in a molten eutectic, lithium-deuteride, thorium or uranium salt at 500°C may provide sufficient thermal energy to melt cryogenic ice while efficiently converting thermal to electric energy to power systems.

MCNP® LCF Fast Fission Modeling

The MCNP® modeling allows determination of the number of fission reactions/second/thermal-watt. This modeling gives rise to the mass/volume/reflectors necessary for the order of 10^{12} fissions/watt. From this result we can derive the model and the power flow diagram, including production of electrical power using the Acoustic Stirling Quad Engine. Furthermore, an understanding of the underlying power output,

would also allow trading off simple thermal melting of the ice by various electrically intensive means, such as augers, ultrasonic, etc.

LCF Fast Fission Reactor Geometry

The base model for this effort was the Kilopower fission reactor. Modifying this model involved using 6.4 MeV source neutrons and 15.0 MeV source protons as described above which can then fission the core material. Varying the core material and neutron reflector design in the model and studying the resulting number of fissions, fission neutrons, and neutrons making it to the ice surrounding the reactor allowed for an optimal design to be developed.

The fusion-fast-fission reactor consists of a reactor core with neutron reflectors to absorb slow neutrons. Those neutrons are from a combination of ^{238}U fast-fission neutrons and the Lattice Confinement Fusion neutrons (6.1 MeV – 6.8 MeV, average 6.4 MeV) as observed by Mosier-Boss et. al. [8]. The MCNP® geometry of the new fusion-

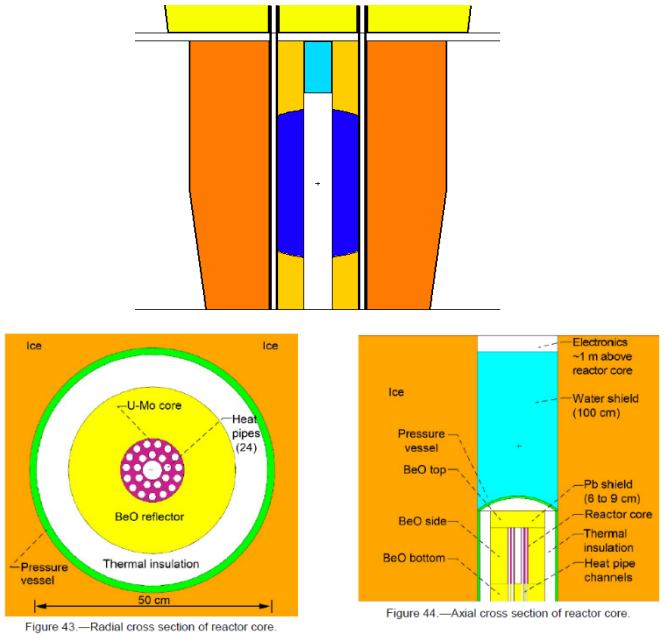

Figure 9. Geometry of the MCNP® Kilopower model.

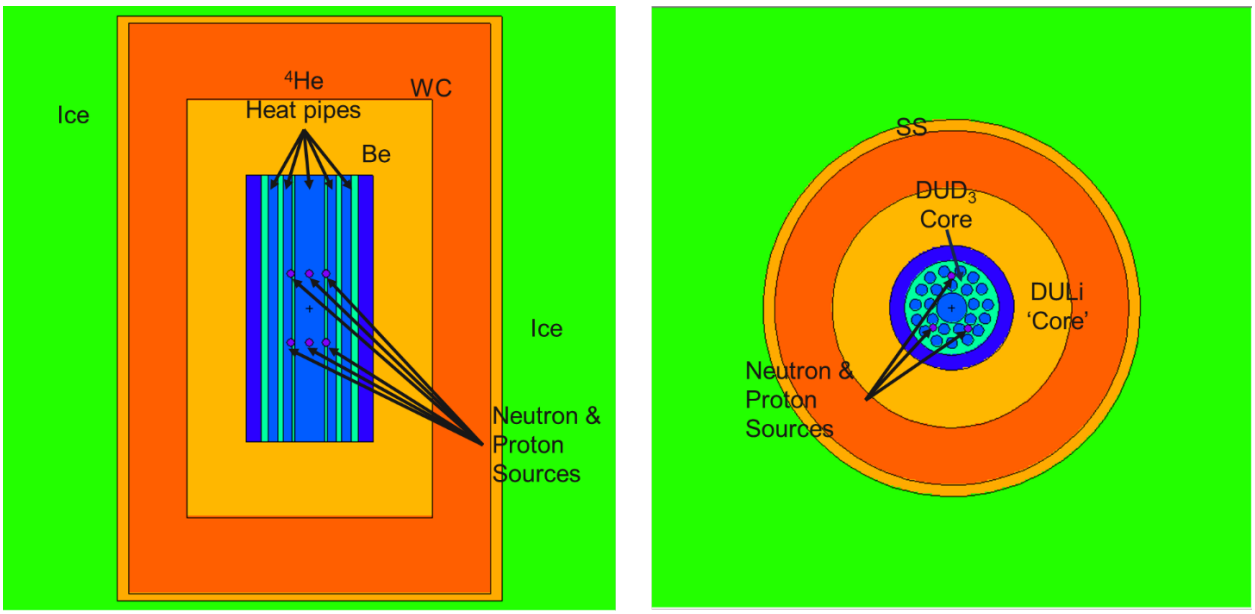

Figure 10. MCNP® Geometry of the LCF Fast Fission reactor design studied.

fission reactor core is shown in Fig 10. One type of reactor core design contains DUD_3 (cyan), and a depleted uranium-lithium (DULi) section (blue) as the reactor core, and a combination of beryllium (orange) and tungsten carbide (dark orange) functioning at the neutron reflectors. In the core, there are 25 total ^{4}He pipes. The configuration of these pipes is such that there is 1 large pipe in the center of the core and 2 sets of concentric cylinders: 9 (inner) and 15 (outer) surrounding the center cylindrical pipe.

These helium pipes (light blue) inside the core help with transferring heat from the core to the surrounding area. The core and reflector assembly are surrounded by a stainless-steel (SS) pressure vessel (orange) which is further surrounded by ice (green) to simulate drilling through an icy crust such as that found on Enceladus. The sources (purple) simulate the products (protons and neutrons) of the Lattice Confinement Fusion reactions.

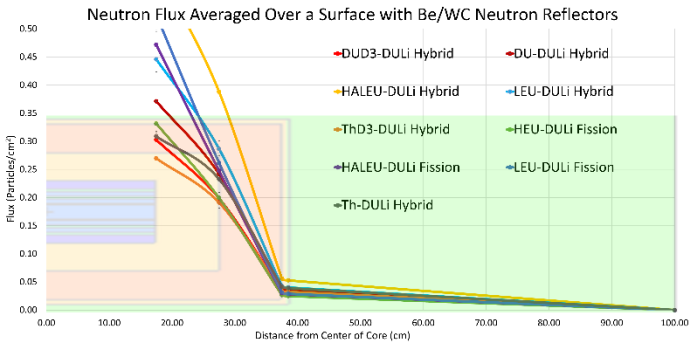

Figure 11. Neutron Flux with Various Reactor Cores as determined by MCNP code calculations.

LCF Fast Fission Reactor Core Material Comparison

MCNP® is unable to model fusion reactions and is restricted to modeling ions with kinetic energy > 1 MeV/nucleon (e.g., 1 MeV protons, 4 MeV alphas). However, it tracks neutrons and their interactions down to thermal energies (e.g., 0.025 eV). These interactions include neutron scattering, or moderation, and capture. For this study, the MCNP® model uses the products of D-D nuclear fusion; 6.4MeV neutrons [8,] and 15.0MeV protons from the subsequent D+^{3}He → p (15.0 MeV) + ^{4}He reaction as shown in the Lattice Confinement Fusion Fast Fission section of this report.

The optimal non-fissile reactor core candidate should produce the most fission reactions in the core (to maximize heat production), the fewest neutrons in the ice (to reduce shielding), and the most tritons in the core (to encourage DT fusion reactions). A multi-pronged approach was carried out to obtain the optimal hybrid fusion fission reactor design. First, the core materials that were modeled with percentages indicating mass percent were:

1) Low-enriched uranium (LEU) consisting of 95% ^{238}U and 5% ^{235}U
2) Highly assayed LEU (HALEU) consisting of 80.45% ^{238}U and 19.55% ^{235}U
3) Depleted uranium (DU) consisting of 100% ^{238}U
4) Deuterated DU (DUD_3) consisting of 97.35% ^{238}U, 0.19% ^{235}U, and 2.46% ^{2}H
5) Deuterated thorium (ThD_3) consisting of 97.52% ^{232}Th, 0.02% ^{230}Th, and 2.46% ^{2}H

Table 3. Comparison of different hybrid reactor core materials with the goal of maximizing the number of fission reactions while minimizing the number of neutrons produced in the ice layer around the hybrid reactor.

Core Material Within SS Vessel	Number of fissions	Fission Neutrons	Neutrons/fission	Tritons in Core	Neutrons in Ice
DUD_3 Hybrid Core	**376,581**	**1,384,787**	**3.68**	**771,913**	**1,326,933**
DU Hybrid Core	547,762	2,030,021	3.71	698,882	1,561,271
ThD_3 Hybrid Core	180,807	655,138	3.62	661,417	1,274,637
LEU Hybrid Core	1,089,459	3,402,934	3.12	693,419	1,827,890
HALEU Hybrid Core	2,440,726	6,846,876	2.81	826,599	2,480,093
HEU Fission Core	22,947,504	58,368,265	2.54	661,429	923,337
LEU Fission Core	30,275,630	77,208,433	2.55	1,138,631	993,832
HALEU Fission Core	28,696,482	73,132,333	2.55	941,173	979,998

These runs were compared to their fission reactor counterparts; LEU, HEU (93.10% ^{235}U, 6.19% ^{238}U, and 0.71% ^{234}U), and HALEU. From these runs, we concluded that the DUD_3 core was the most effective in terms of lowest number of neutrons in the reactor SS shielding (Fig 11) and the highest number of fission reactions comparing the non-fissile material cores (DUD_3, DU, and ThD) with the fissile cores (LEU, HALEU, and HEU). The results of these runs are shown in Table 3 where 2 million 6.4 MeV neutrons and 2 million 15 MeV protons were used as the source particles.

In addition to modeling different core materials, we investigated different neutron reflector materials surrounding the reactor core. The reflectors that were modeled were:

1) Beryllium (Be)
2) Tungsten (W)
3) Titanium Carbide (TiC)
4) Tungsten Carbide (WC)
5) Magnesium Oxide (MgO)
6) Combination Be (inner reflector) and WC (outer reflector)

From the reflectors modeled above, the Be and WC combination yielded the best compromise between most fission reactions and the least number of escaped neutrons as listed in Table 4.

Table 4. Comparison of different neutron reflectors with the DUD_3 core and run with 4 million particles.

Core Configuration	Number of fissions	Fission Neutrons	Neutrons in core	Tritons in core	Neutrons in Ice
DUD_3 Core with TiC Reflector	470,468	1,722,256	10,202,007	370,061	1,841,045
DUD_3 Core with W Reflector	466,984	1,714,135	7,473,623	258,788	1,537,265
DUD_3 Core with MgO Reflector	451,934	1,674,443	9,301,039	169,518	2,303,200
DUD_3 Core with Be Reflector	518,205	1,842,370	7,888,964	1,415,672	2,247,560
DUD_3 Core with WC Reflector	473,419	1,731,488	7,423,115	286,794	1,016,188
DUD_3 Core with Be/WC Reflectors	376,581	1,384,787	7,144,690	771,913	1,326,933

Analyzing the MCNP® Calculations

Working further with the DUD_3/DULi reactor core and the surrounding beryllium (Be) and tungsten (W) reflectors reveal the possible reactions especially within the core that validates the heat generated from this design. The results from the MCNP® runs offer a multitude of data that can determine the types of reactions that would occur within our LCF Fast Fission reactor model. The most important type of data is the photon spectra within the modeled reactor core which indicates the reactions that are occurring determined by the MCNP® calculations. Figure 12 shows the photon flux within the DUD_3 reactor core. There are several peaks indicating that there were several reactions taking place within the DUD_3 core. With the help of PeakEasy [32], peaks were identified, and the subsequent reactions were verified in the Nuclear Energy Agency's Java-based nuclear information software (JANIS) tables [33]. Analyzing this spectrum reveals that many different reactions can occur in this core such as:

1) $^{9}Be(n,\gamma)^{10}Be$ (Fig 13): Neutron capture of beryllium
2) $^{9}Be(\alpha,n)^{12}C$ (Fig 14): Alpha capture of beryllium
3) $^{186}W(n, \gamma)^{187}W$ and $^{182}W(n, \gamma)^{183}W$ (Fig 15): Neutron capture of tungsten

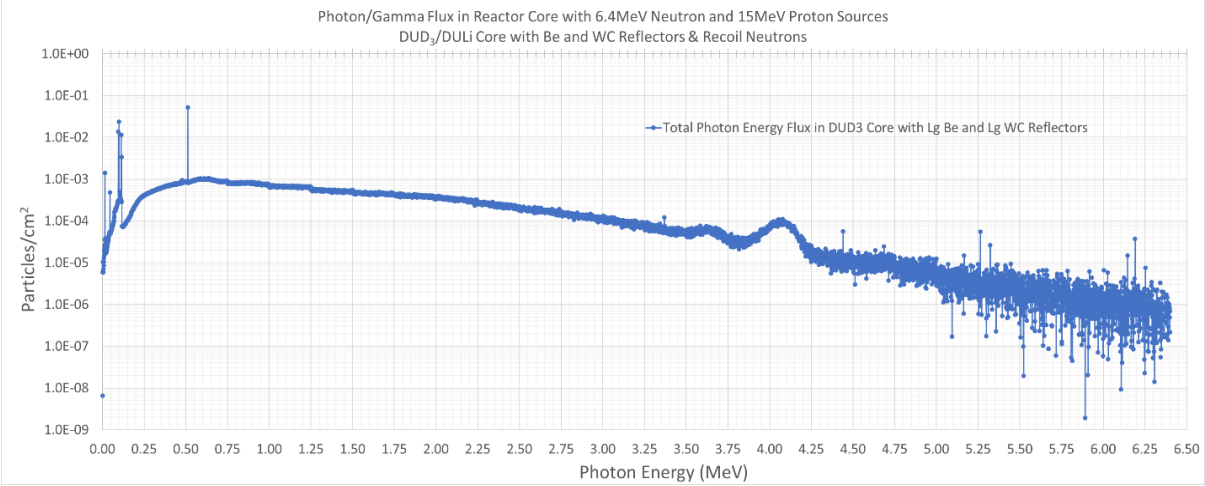

Figure 12. Photon flux inside the DUD_3 reactor core from the MCNP® calculation of the LCF Fast Fission Power Reactor design based on the Kilopower Reactor.

4) U(x-rays) (Fig 16): Natural x-ray decay of uranium
5) ^{240}Pu (Fig 17): Neutron capture and decay chain: ^{238}U > ^{239}U > ^{240}U > ^{240}Np
6) ^{89}Sr (Fig 18): Fission product of uranium; strontium
7) ^{134}I (Fig 19): Fission product of uranium; iodine
8) ^{133}I (Fig 20): Fission product of uranium; iodine

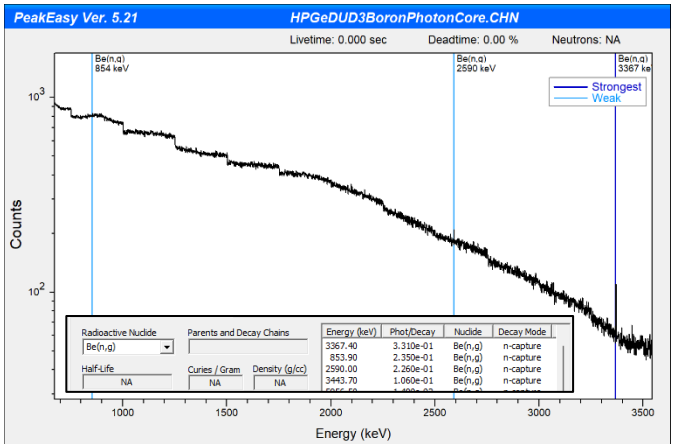

Figure 13. Part of gamma spectra showing the ^{9}Be(n,γ)^{10}Be reaction.

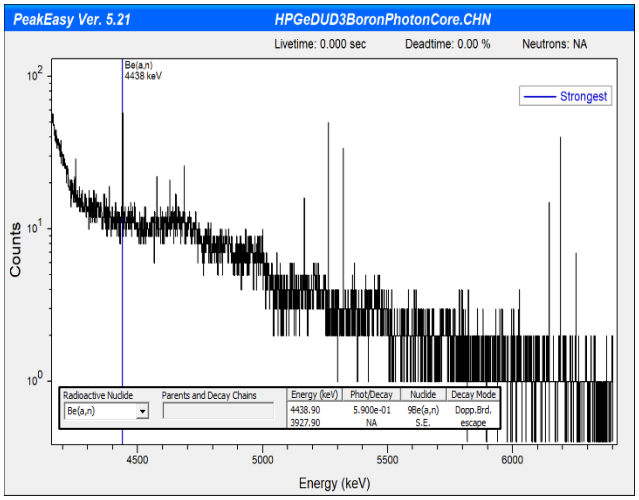

Figure 14. Part of gamma spectra showing the ^{9}Be(α,n)^{12}C

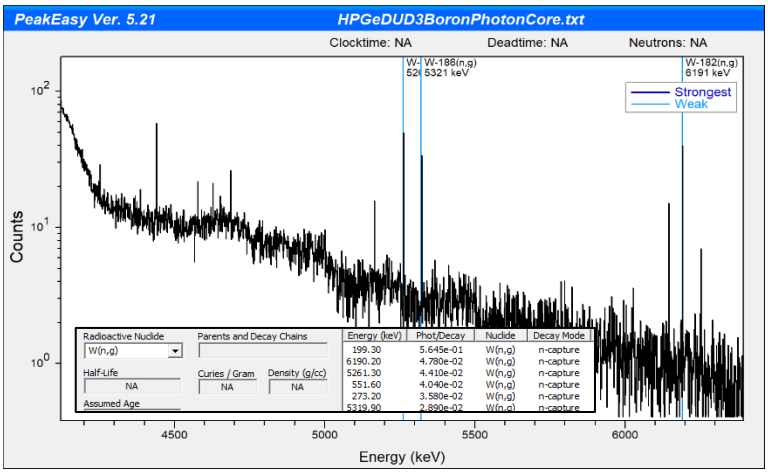

Figure 15. Part of gamma spectra showing the $^{186}W(n, \gamma)^{187}W$ and $^{182}W(n, \gamma)^{183}W$ reactions.

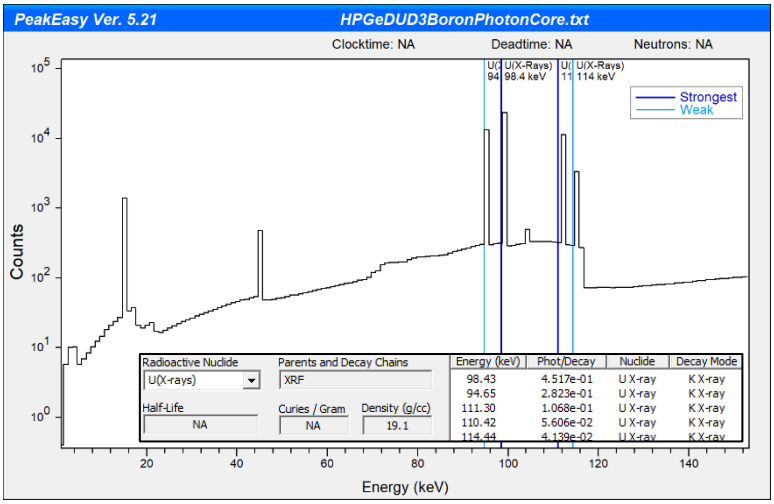

Figure 16. Part of gamma spectra showing the peaks of U(x-rays).

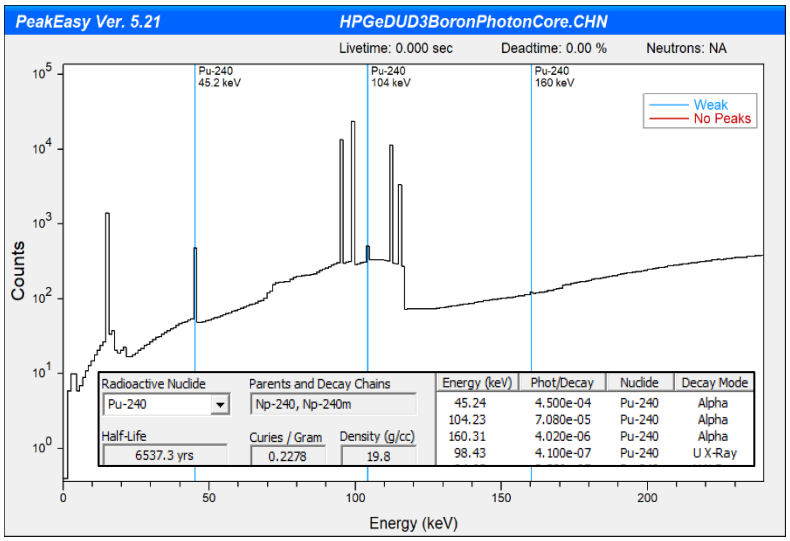

Figure 17. Part of gamma spectra showing peaks of the ^{240}Pu isotope.

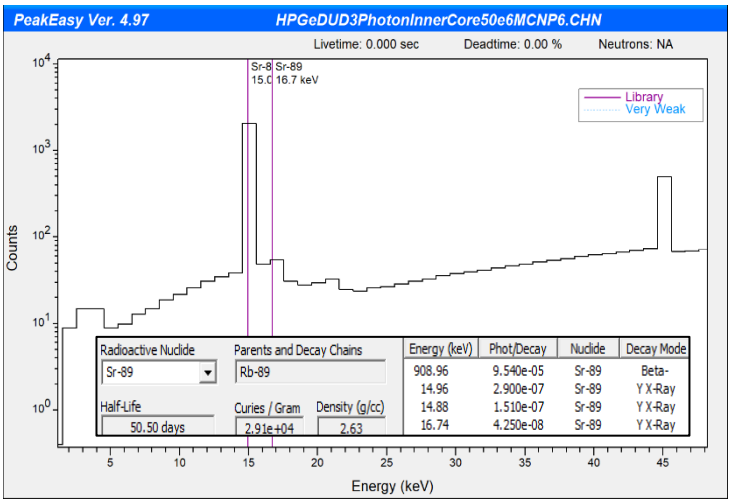

Figure 18. Part of gamma spectra showing peaks of ^{89}Sr; a fission product of uranium.

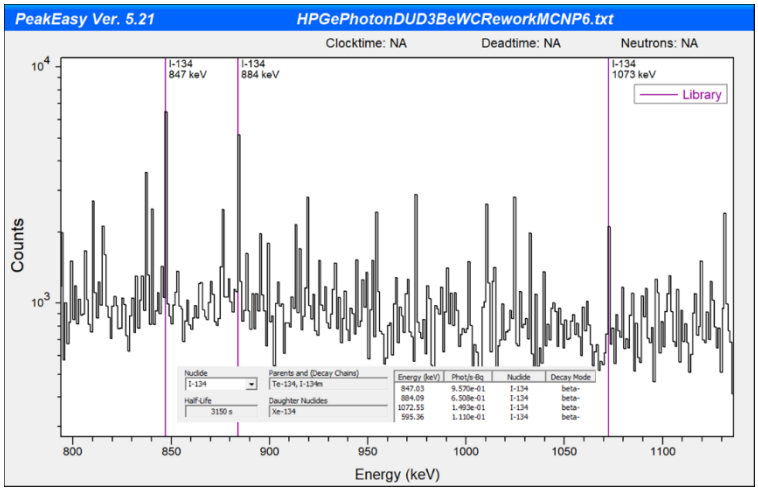

Figure 19. Part of MCNP® gamma spectra showing the ^{134}I fission product's strongest gamma peaks.

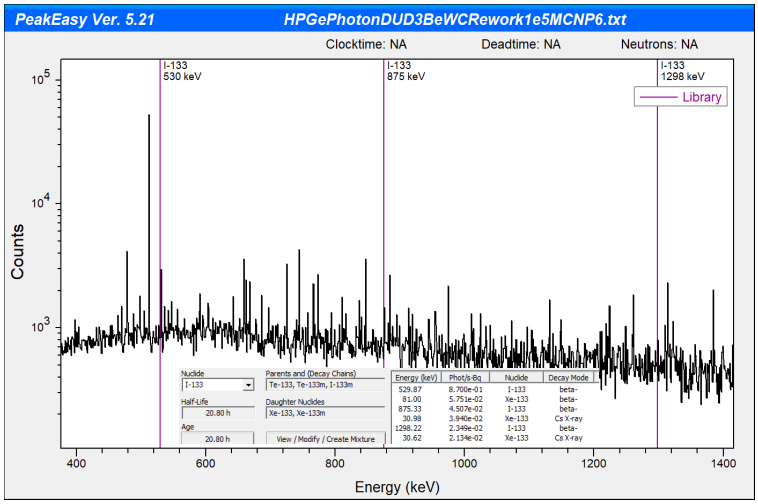

Figure 20. Part of the MCNP® gamma spectra showing the ^{133}I fission product's strongest gamma peaks.

Hybrid Fusion Fission Reactor Power Determination

Determining the power output of the newly modeled hybrid reactor involves the size and composition of the reactor. The dimensions of the MCNP®-modeled hybrid reactor are like the Tunnelbot's reactor design as shown in Fig 9 where the inner reactor core is 13cm in diameter with an overall vessel diameter of 50cm. The length of the reactor core is 35cm with an overall length of the pressure vessel of 77cm. The pressure vessel contains the reactor core. Fig 10 shows the MCNP® geometry of the optimal design of the hybrid reactor. The dimensions of the proposed hybrid powered reactor are taken from the Europa Tunnelbot design and the newly designed hybrid reactor and are listed in Table 5. The resulting volume and weight of just the reactor core (DUD_3 and DULi) are 5.6L and 59.2kg. Comparing to other fission core materials, the reactor core weights do not change very dramatically where the HEU/DULi core is 77.6kg, the LEU/DULi core is 77.9kg, and the HALEU/DULi core is 77.9kg. In addition, as compared to the overall size of the Tunnelbot vehicle for example, the hybrid LCF Fast Fission Reactor is 1.75 times smaller than the Kilopower Reactor.

Table 5. Component dimensions of LCF Fast Fission Reactor.

	Hybrid Fusion Fission Reactor
Inner Core Material	Deuterated Depleted Uranium
Radius	6.25 cm
Length	35 cm
Volume	2,370.9 cm^3
Heat Pipes within Inner Core	Helium-4
Length	35 cm
Volume	1,924.2 cm^3
Outer Core Material	Depleted Uranium-Lithium
Outer Radius	8.25 cm
Thickness	2 cm
Length	35 cm
Volume	3,188.7 cm^3
Inner Neutron Reflector	Beryllium
Outer Radius	15.25 cm
Thickness	8.25 cm
Length	55 cm
Outer Neutron Reflector	Tungsten Carbide
Outer Radius	23.5 cm
Thickness	8.25 cm
Length	75 cm
Pressure Vessel	Stainless Steel
Outer Radius	25 cm
Thickness	1.5 cm
Length	77 cm
Total Volume of Reactor Cores	5.56 L or 5,559.6 cm^3
Total Weight of Reactor Cores	77.8 kg

Fusion Fast Fission Nuclear Cascade

A conventional fission chain reaction (Fig 21) requires neutrons produced via fission that are moderated to thermal energies (.025 eV) allowing neutron multiplication. Uranium (^{235}U) and plutonium (^{239}Pu) have large fission cross-sections (>500 barns for moderated neutrons), resulting in high probabilities of fissioning. The peak fission neutron kinetic energy is 750 keV to 1 MeV and the average 2 MeV. Depleted uranium ^{238}U is almost 1000 times more likely to elastically scatter a neutron (8 barns for a 1 MeV neutron) vs only 10 millibarns (mb) for fission at that energy. Consequently, ^{238}U is unable to sustain a chain reaction. It will more efficiently fission with neutrons over 2 MeV, like 2.45 MeV fusion neutrons.

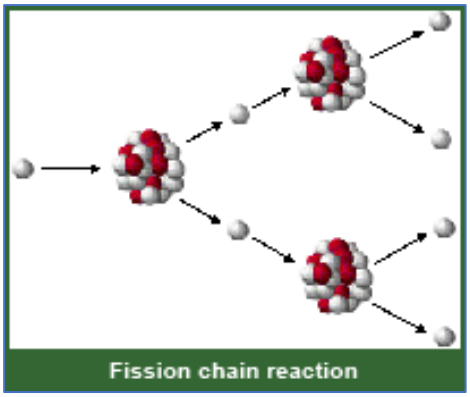

Figure 21. Typical fission chain reaction.

Neutrons that elastically scatter off a ^{238}U nucleus will lose less than 0.5% of their energy due to the 238:1 mass difference between uranium and a neutron. The fission neutrons won't fission ^{238}U but they can transfer 4/9 of the neutron's kinetic energy to a deuteron due to their similar masses (1:2).

- $D(d,n)^3He$ produces a 2.45 MeV neutron, n.
- The fusion neutron fissions $^{238}U(f,2+n)$ producing 2+ neurons and fission products

A NASA Patent Disclosure has been filed with the Glenn Research Center as LEW-20878-1, "Method for A Nuclear Fusion-Fission-Fusion Cascade"

Neutron Mean-Free Path

A neutron's mean-free path is the average distance it can travel depending upon its energy, the density of the material and its various scattering and capture cross-sections. We calculate the neutron mean-free path in DUD_3 to be 3.5 mm which is comparable to a neutron's mean-free path in a conventional fuel rod. This holds for neutrons from 50 keV to 3 MeV.

Deuteron Fuel Density

Two uranium hydride (UH_3) structures are identified, but with a slightly lower density than DUD_3. Using the UC Berkley Materials Project [35] data the UH_3 (mp-24669) spacing has a volume of 73.35 $Å^3$ consisting of four 2.32 Å and eight 2.35 Å UH bonds. This crystallizes as a tetragonal P42/mmc space group. Using these values, each deuteron will be within roughly 2.3 Å x 2 of each other in edge, face and edge-sharing cuboctahedra, or 4.6 Å of each other.

Fusion

Each completed fusion reaction produces 24 MeV with 2/3 leaving as neutron kinetic energy where "p" is a proton, "n" a neutron, "D" and "d" are deuterons, "T" and "t" are tritons, "^{3}He" is a helion,

D(d,n)^{3}He	with a 2.45 MeV neutron, 1 MeV 3He
D(d,p)T	with a 3 MeV proton, a 1 MeV triton
D(^{3}He,p)alpha	with a 14.7 MeV proton, and a 3.6 Mev alpha
D(t,n)alpha	with a 14.1 MeV neutron and a 3.5 MeV alpha

In conventional hot fusion the D(d,p)T channel breeds tritium which can participate with a 100x higher fusion cross-section than deuteron-deuteron fusion. Despite the inability to model fusion, our MCNP modeling found tritium is bred through interactions with Li and n capture on deuterons. The fast neutrons will fission ^{238}U, as will the 15 MeV protons, though not efficiently.

Fast Fission

Both the 2.45 MeV and 14.1 MeV neutrons will fission ^{238}U. Each fission reaction results in 190+ MeV of kinetic energy in the fission products including fast neutrons.

Neutron capture and slow fission

Side reactions that build over time include the neutron capture and decay chain: ^{238}U > ^{239}U > ^{239}Np > ^{239}Pu. Although ^{238}U is fertile, not fissile, it can result in fissile ^{239}Pu. There are competing processes for ^{239}Pu. Fast neutrons will equally fission ^{239}Pu and ^{238}U with cross-sections of 1 – 2 b. Each of these fissions liberates 190+ MeV, whether a higher cross-section thermal fission of ^{239}Pu or a fast fission.

Power Determination

Lifetime

The major energy source in Lattice Confinement Fusion Fast Fission is ^{238}U fission providing approximately 200 MeV/fission. One thermal watt requires 3.1 x 10^{10} fissions/second. Our goal is to generate 12 kWt, or the equivalent of 4 x10^{14} fissions/second with a lifetime of 10 years. There are 3x10^8 seconds in a decade. Therefore, we would need 12x10^{22} total fission reactions. Thus, we would need sufficient DUD_3 to produce 10^{23} fissions and a comparable number of fusion reactions to drive it.

The proposed core consists of 59.2 kg. The density of DUD_3 is 11.11 g/cm^3 whereas DULi density is 10.31 g/cm^3. Both materials can sustain fusion fast fission with Li providing a source of tritium in addition to tritium produced by neutron capture in DUD_3. Given a core of 59.2 kg (6 x 10^4 grams) with an average density of 11 g/cm^3 with a resulting volume of 5,454 cm^3, with a molar mass of 244 g/mole, there are about 246 moles of DULi and DUD_3 which corresponds to 6.023x10^{23} atoms/mole or 15x10^{25} atoms in the reactor which means there are 375x10^{23} DU atoms in the reactor. With the number of fission reactions needed in the 10-year duration, we'll burn up about 31% of the DU fuel.

MCNP Modeled Fission

The table below shows the MCNP® results of the DUD_3 hybrid core driven by 4x10^6 boosted 6.4 MeV fusion neutrons induced 13% of the modeled fissions. MCNP® cannot capture the fusion reactions induced by most of the input neutrons. It is notable that despite the relatively small deuteron capture cross-section there are nearly twice as many tritons as fissions. There is sufficient energy in each of the 6.4 MeV neutrons as experimentally measured [15,27] to induce multiple fission reactions.

Number of fissions	Fission neutrons	neutrons/fission	Tritons in core
507,975	1,816,902	3.58	932,269

The neutrons have a mean free path of 3.5 mm in DUD_3 and will heat deuterons and the deuterons will fuse, just before the Bragg Peak at 7 mm, producing more fast neutrons to fission the ^{238}U. MCNP is unable to track fusion reactions or light nuclei and misses the following reactions:

1. All fusion reactions producing 2.45 MeV and 14.1 MeV neutrons, and fast protons
   a. These fission ^{238}U and/or heat deuterons to fusion.
2. Fission neutrons scatter off deuterons < 2 MeV.
   a. These heat deuterons inducing fusion.

Table 3 indicates each fast LCF fission results in 3.58 neutrons that in turn can induce as many fusion reactions as possible which in turn will either heat adjacent deuterons or fission ^{238}U, releasing more neutrons to heat additional deuterons. In addition, it takes as little as 5 keV/deuteron to heat it to fusion temperatures. A 2 MeV average energy fission neutron will lose 4/9 of its energy with each deuteron encounter and less than 0.5%, or 100 keV, to ^{238}U scattering. Hence multiple deuterons will be heated by each fission neutron with the first deuteron acquiring up to 0.9 MeV.

Power Gain

Given the neutron mean free path in DUD_3 of 3.5 mm, each of the fission neutrons will encounter one or more deuterons transferring energy. A 2 MeV fission neutron has a velocity of 2 x 10^7 m/sec (20 mm/msec). It will traverse 3.5 mm in 6 msec where it would encounter a deuteron and drive it to fusion. The fusion reaction is strong force enabled and happens effectively instantaneously. A 2.5 MeV fusion neutron will travel at approximately the same rate and traverse 3.5 mm in 6 msec. Therefore, each fission>fusion>fission cascade will take 12 msec on average.

The doubling time number of generations (N) used in fission reactions where k is the reproduction constant:

N=ln 2/ln(1.+ k) number of generations to double the reaction rate. Here, k=.012 s.

Therefore, N= 0.70/0.012 = 58 generations, or a doubling time of (58)(.012)=0.69 seconds. Each reaction consists of a deuteron-deuteron fusion pair, (4 MeV), plus ^{238}U fission (200 MeV). Therefore, each generation number of reactions times 204 MeV, is the energy produced in that generation:

Generation	Energy (eV)	Number of fissions
50	7.96E+22	3.90E+14

By the 50th generation, Lattice Confinement Fusion fast fission in this configuration has reached 12 kWt/sec. Without interruption, it will reach the 50th generation in 34.5 seconds. This type of configuration is controllable and could be modeled with a Markov chain.

Rate limiting factors:

thermal: reactor has a negative thermal coefficient, as it heats the deuterons move away from the current active sites.

Screening: as the kinetic energy exceeds 10 keV screening no longer plays a role in enhancing fusion

Fuel density: related to thermal and screening, as the lattice expands the fuel density drops and with it the electron density providing nuclear shielding.

Product poisoning: fusion produces alphas that will fill interstitial spaces preventing deuteron occupancy and consequently fusion reactions. Alphas are a fusion "ash". This is like fission poisoning but that relates to thermal fission poisons like ^{135}Xe with a thermal neutron capture cross section of 2.0×10^6 barns. Lattice confinement fusion doesn't depend upon thermal neutrons.

Energy Conversion

The power generated by the LCF Fast Fission Reactor will then to be converted into useful electrical power and heat for helping to keep components warm within the robotic probe and help melt the ice around the probe. An Acoustic Stirling Quad Engine [28-30, 34] can be used for electric generation from a low temperature 24 kW_{th} hybrid fusion-fast fission reactor heat source to generate a 4 kW_e power output with 20 kW_{th} thermal output for external ice phase management. A special subset of Stirling engines based on thermoacoustics is shown in Fig. 22. The thermoacoustic Stirling Engine either generates a sound wave with thermal input or it can operate in reverse to provide refrigeration using the energy from an incoming acoustic wave. The acoustic wave can generate electric power by either extracting the pressure wave with an oscillating piston, or for higher power levels it can extract the velocity wave with a bi-directional turbine as shown in Fig. 23.

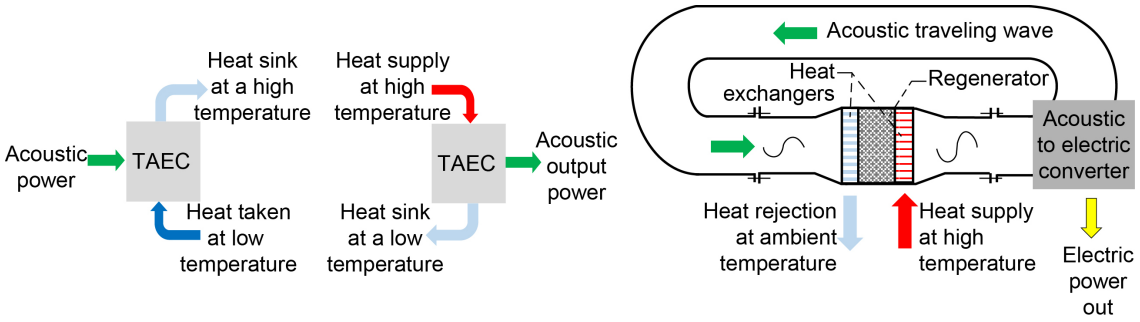

Figure 22. Acoustic Stirling Fundamentals

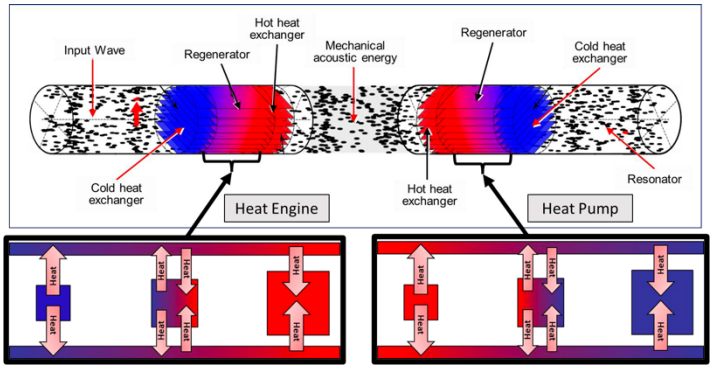

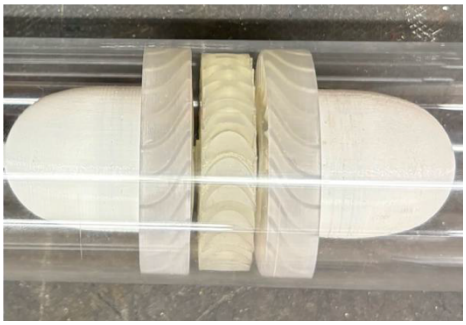

Formlabs Form 3L, Clear Resin V4 (2117 RPM)

Figure 23 Thermoacoustic Power with Bi-Directional Turbines [34]

Heat Exchangers

Traditional heat exchangers can be replaced with acoustic heat exchangers as shown in Fig. 24. Each heat exchanger has a hot and cold side separated by a regenerator. A portion of the hot input energy is converted to an acoustic wave and the remaining is transferred to the cold side acoustically.

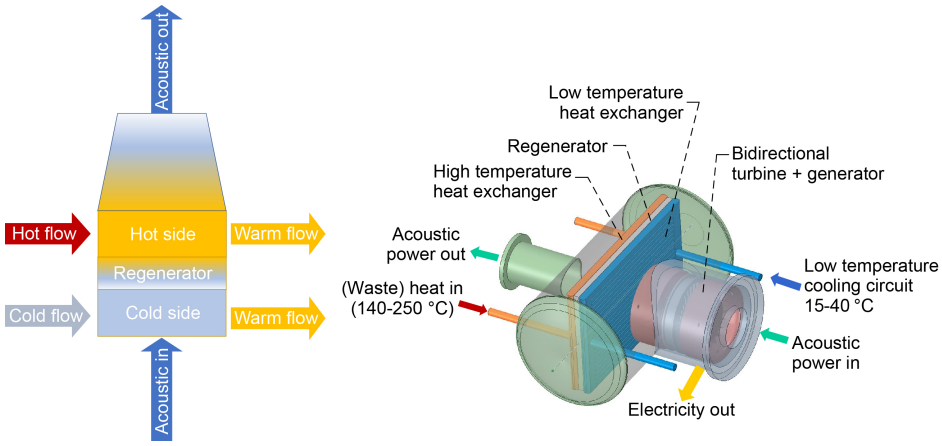

Figure 24. Oscillating heat pipes transport thermal energy from/to the acoustic Stirling heat exchangers

Oscillating heat pipes (OHP) facilitate the transfer of heat from the heat source to heat exchanger and likewise from the cold heat exchanger to the lower temperature cold sources such as the immersed robotic probe in an icy environment. The minimum delta T possible for the acoustic Stirling is rather small at 100° C as shown in Fig. 25 compared to other power conversion technologies. This low delta T enables the use of a molten salt Lattice Confinement Fusion reactor which may operate at 300 C or below to

achieve a conversion efficiency of 20%. At these low operating temperatures, this precludes the use of solid-state thermoelectric and thermionic power conversion technologies. The rejected waste heat is then transported via no-moving part oscillating heat pipes for external ice phase management.

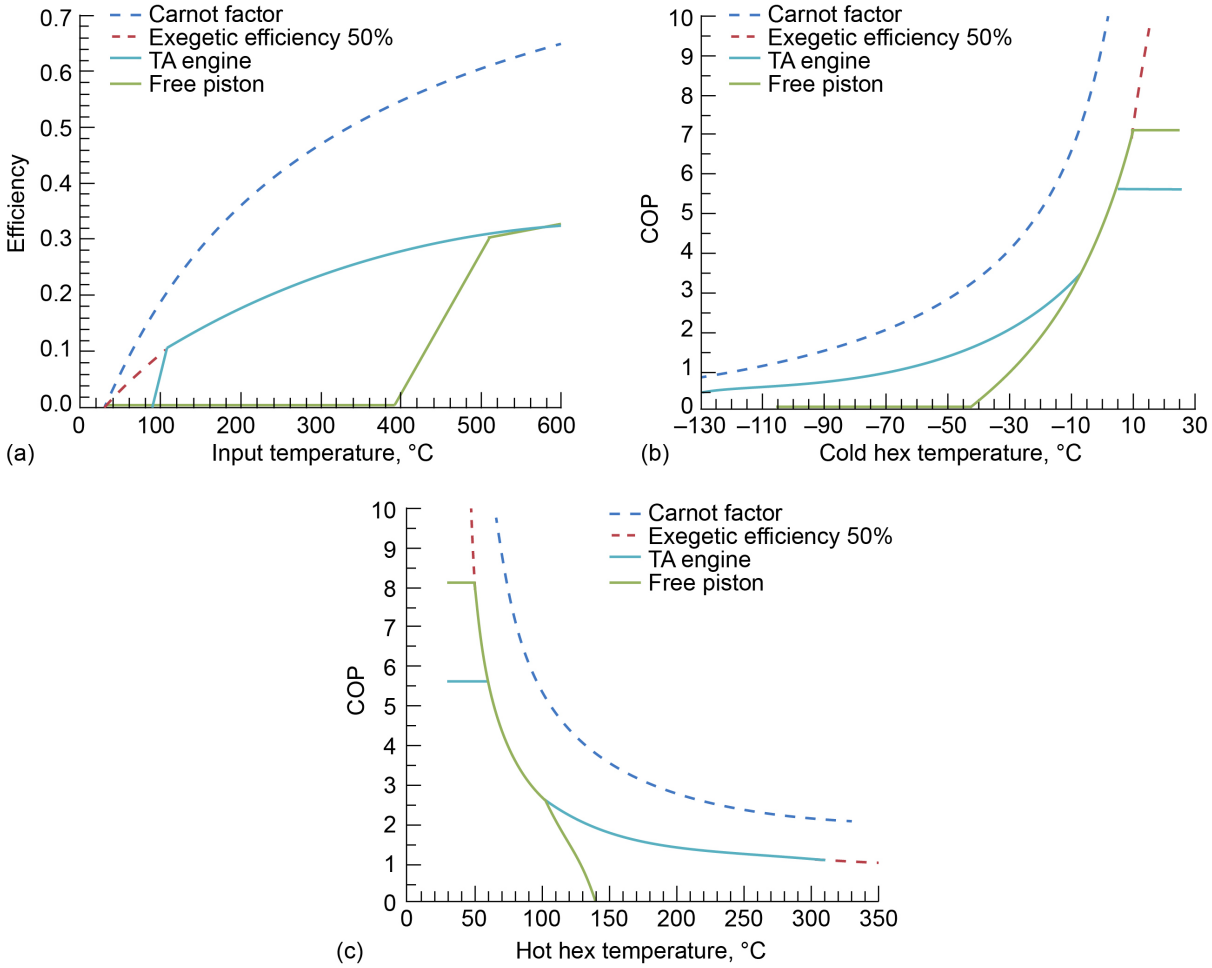

Figure 25. Ring of thermoacoustic heat exchangers with oscillating heat pipes (OHP) surrounding a heat source such as from a hybrid fusion fission reactor.

Four of these acoustic heat exchangers are placed ¼ wavelength apart to form a self-amplifying acoustic loop as shown in Fig. 26. The acoustic energy in the loop can be used to generate electricity with a bi-directional turbine generator.

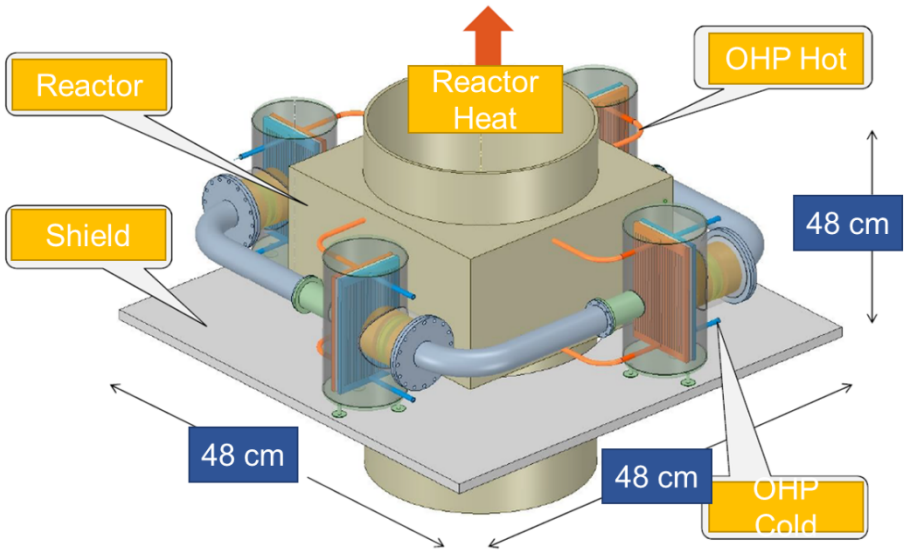

Figure 26. Ring of thermoacoustic heat exchangers with oscillating heat pipes (OHP) surrounding a heat source such as from a hybrid fusion fission reactor.

Traveling Through the Ice

A hybrid system that cuts, drills, heats, and vibrates the ice will be designed to optimize the speed through which the probe travels through the ice. The components consist of the following: a drill/auger which grinds up the ice, an ultrasonic heated blade which melts the ice and vibrations to help break up ice after heating, and rear electrically heated fins which "cut" through the ice and provides drag stabilization, counter-torque for the drill, and differential drag for steering.

It is recognized that communicating through 20 – 40 km of ice is the most serious, unresolved, problem with attempting this type of exploratory mission. One solution has been to place ^{238}Pu "pucks" to produce repeater-power tethered together with a fiber optic cable. It is recognized this may not work due to shifting ice between the probe and the surface. Consequently, various RF, magnetic, and acoustic solutions have been suggested and some tried. Unfortunately, it is recognized that high power budgets may be necessary to propagate an electromagnetic, magnetic, or acoustic wave through the ice. This would seriously change the instrumentation/communications power budget.

Protecting Lifeforms Encountered Under the Ice

Nuclear-powered probes searching for extraterrestrial life on Icy Worlds need to consider environmental nuclear activation just as may occur with terrestrial nuclear-powered vessels. The Los Alamos National Laboratory (LANL) MCNP® nuclear modeling code was used to calculate these effects as outlined in a white paper [31] regarding the Saturnian icy moon, Enceladus. Experimentally, this can be assessed using a spontaneous fission source, like californium ^{252}Cf.

Icy outer planet worlds are suspected to have sub-surface oceans but with up to 40 km of ice cap over them. Nuclear radioisotope, ^{238}Pu, and fission powered probes [6] have been proposed to spend three or more years traversing the ice caps. Not well known, is that the production of ^{238}Pu contains various plutonium isotopes, some of which are fissile. Also, the energetic alphas unexpectedly induce (alpha,n) reactions among various shielding and probe components.[37]

The Saturnian moon, Enceladus, and the Earth's oceans contain salts, including sodium chloride. One of the chlorine radioisotopes has an activated half-life of 38 minutes. For each half-life the residual amount is cut in half. Seven half-lives leave only 1% of the original amount which would be detectable for over 4 hours after production. Decays of ^{38}Cl through two paths seen below showing the gamma (γ) energy, the intensity/decay, the decay mode, half-life and the parent. The γ energy is in keV, or thousands of electron volts. The intensity, Ig, indicates the proportion of each decay's energy. The decay mode, IT, is an internal nuclear transition first step whereas b- (β-) is a beta decay 2nd step resulting in ^{38}Cl(β-,γ)^{38}Ar, which is stable.

Eg (keV)	Ig (%)	Decay mode	Half life	Parent
671.355	99.95 *1*	IT	715 ms *3*	^{38m}Cl
1642.714	31.9 *10*	b^-	37.24 m *5*	^{38}Cl
2167.405	42.4 *11*	b^-	37.24 m *5*	^{38}Cl

Except for neutron capture resonances, neutron capture follows a 1/v capture cross-section where v is the neutron's velocity and hence it's kinetic energy. Hence reflectors and absorbers preferentially redirect then capture slow neutrons. A combination beryllium and tungsten system of neutron reflectors

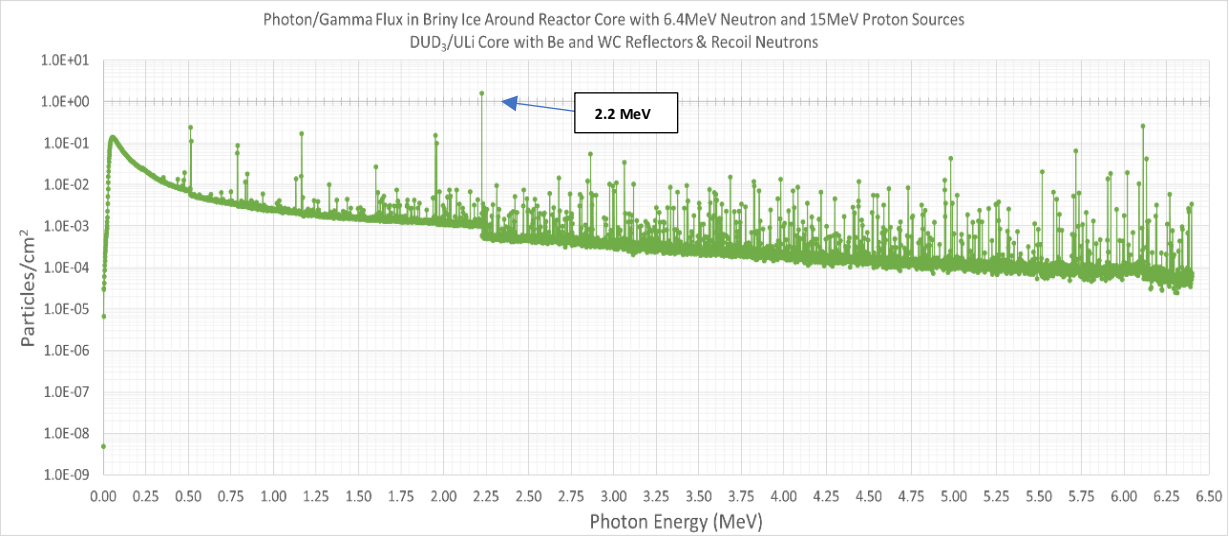

Figure 27. MCNP® Modeled Gamma Spectra in Briny Ice

have been included in the MCNP® modeled developed in this study. Nonetheless, fast neutrons will thermalize and be captured within the ice and the sub-surface ocean. Fortunately, this thermalization will reduce the environmental fast neutron flux by $1/r^2$, as a larger area and consequently fewer neutrons will irradiate a given area at distances r as compared to an immediately captured thermal neutron. The overall seawater activation is the integral of the neutron scatter, or moderation, water cross-section, σ_s, the specific isotope activation capture cross-section, σ_c, the isotopes' densities, ρ, and the prompt and half-life delayed gammas. These can be calculated from MCNP®. Neutron capture on hydrogen in H_2O is a prompt reaction: H(n,γ)D, resulting in a 2.223 MeV gamma ray, (Figure 27) and becomes a deuteron. Similar reactions occur with the stable isotopes of oxygen. Figure 28 shows the MCNP® synthetic spectra interpreted using the Los Alamos National Laboratory's PeakEasy code [31] that identifies gamma peaks from their corresponding tabulated energies. In this case, the neutron activation of a stable chlorine isotope in seawater by the reaction ^{35}Cl(n,γ)^{36}Cl which has a half-life of 300,000 years. Other than prompt

gammas upon neutron capture the long half-life would make its decay undetectable. Many of the lines are from chlorine isotope activation. Others are gamma lines from the fission, core and shielding activation and activation of the seawater ice.

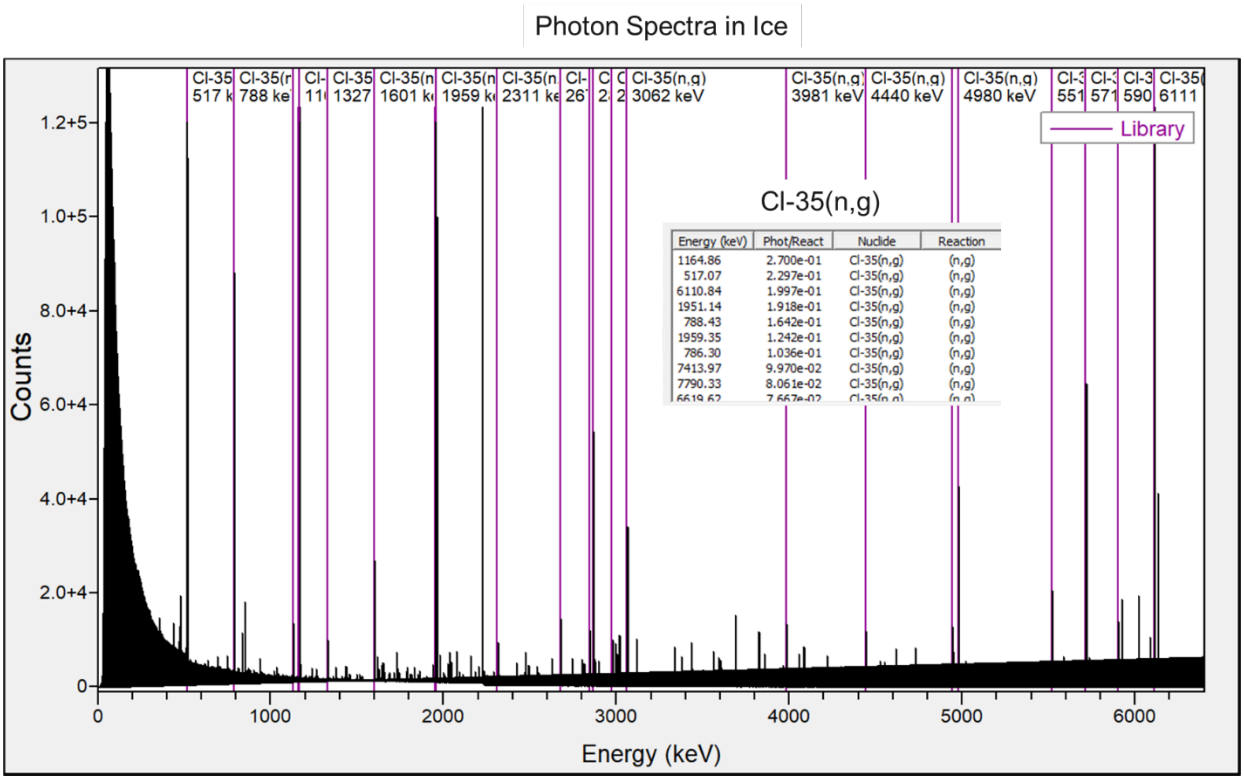

Figure 28. MCNP® synthetic gamma spectra to 6.4 MeV with partial PeakEasy line identification showing seawater chlorine activation, istotope $^{35}Cl(n,\gamma)$ spectra

Further study to establish shielding that will protect the potential lifeforms that the autonomous robotic probe may encounter is necessary.

Summary

In this study, it was determined that a hybrid fusion fission reactor is a safer alternative to traditional fission reactors. The proposed innovation is a compact, scalable nuclear energy source that does not use highly enriched uranium (HEU), high-assay enriched uranium (HALEU), low enriched uranium (LEU) nor plutonium-238 (^{238}Pu). The nuclear energy source consists of a hybrid fusion-fast-fission method whereby neutrons generated from LCF are used to fission materials such as depleted uranium or thorium. The Monte-Carlo modeling environment MCNP was used to model a hybrid fusion fission reactor based on the previously designed and built Kilopower Fission Reactor which uses enriched uranium materials. Several reactor core material combinations were executed under MCNP® and the optimal hybrid reactor design consisted of DUD_3 for the inner reactor core, DULi for the outer reactor core with layers of beryllium and tungsten carbide surrounding the core. The resulting MCNP model yielded the best combination of fission neutrons, tritium production, and low neutron production outside of the SS enclosed vessel. While LCF has been demonstrated by both NASA and Lawrence Berkeley National Laboratory, a hybrid LCF fast fission still needs to be fully demonstrated. Using the hybrid reactor designed here, future work could involve experimentally investigating the practical use of an LCF Fast Fission Reactor.

While this study strived to minimize the neutrons making it to the outside of the hybrid fusion fission reactor, Icy World probes need to consider the issue of minimal shielding due to vessel size in sea water. It is noteworthy that both prompt and delayed gamma activation occurs due to neutron capture in the environment. High energy photons, neutrons, protons, and alphas can induce secondary reactions especially in briny ice and seawater of icy worlds. These energetic particles could kill extraterrestrial organisms or denature biomolecule signatures of their presence. Hence, developing nuclear reactions with a minimal radiation footprint is necessary. The Lattice Confinement Fusion Fast Fission system may be capable of generating power with minimal escaping neutrons and gamma rays.

References

1. https://science.nasa.gov/science-at-nasa/ocean-worlds-the-search-for-life
2. https://en.wikipedia.org/wiki/Ocean_Worlds_Exploration_Program
3. Steinetz, B., T. L. Benyo, A. Chait, R. C. Hendricks, L. P. Forsley, B. Baramsai, P. B. Ugorowski, M. D. Becks, V. Pines, M. Pines, R. E. Martin, N. Penney, G. C. Fralick, C. E. Sandifer II, "Novel nuclear reactions observed in bremsstrahlung-irradiated deuterated metals", *Phys Rev C*, **101**, 044610 (2020). https://doi.org/10.1103/PhysRevC.101.044609.
4. Schenkel, T., et al., "Investigation of light ion fusion reactions with plasma discharges", J. Appl. Phys, 126 (2019) 203302. https://doi.org/10.1063/1.5109445
5. https://www.astralsystems.com/technology
6. Oleson, S., Newman, J. M., Dombard, A., Meyer-Dombard, D'A., Craft, K., Sterbentz, J., Colozza, A., Faller, B., Fittje, J., Gyekenyesi, J., Jones, R., Landis, G., Lantz, N., Mason, L., McCarty, S., McKay, T., Packard, T., Schmitz, P., Turnbull, E., and Zakrajsek, J., "Compass Final Report: Europa Tunnelbot", *NASA/TP*—2019-220054 (2019).
7. Vanek, B., "Control methods for high speed supercavitating vehicles", *Ph.D Thesis*, University of Minnesota, (2008). https://www.semanticscholar.org/paper/Control-Methods-for-High-Speed-Supercavitating-Vanek/0e7325ad5a1f035eb82a34bd4aa2c5cb1e6c84f8
8. Hockman, B., Smith, M., Howell, S., et al., "PRIME: Probe using Radioisotopes for Icy Moons Exploration - A Comprehensive Cryobot Architecture for Accessing Europa's Ocean" in AGU Astrobiology Science Conf. Abstracts. May 2022. https://agu.confex.com/agu/abscicon21/meetingapp.cgi/Paper/1028536
9. JASON, "Prospects for Low-Cost Fusion Development", MITRE Corporation, JSR-18-011, ARPA-E Project 1318JAPM (November 2018). https://fas.org/irp/agency/dod/jason/fusiondev.pdf
10. https://www1.grc.nasa.gov/space/science/lattice-confinement-fusion/
11. Pines, V., et al., "Nuclear fusion reactions in deuterated materials", Phys Rev C 101 (2020) 1044609. https://www1.grc.nasa.gov/wp-content/uploads/TP-20205001617-Theory-Paper-Final.pdf
12. M. Lipoglavšek and Mikac, U., "Electron Screening in Metals", AIP Conf. Proc., 1377 (2011) 383. http://dx.doi.org/10.1063/1.3628420
13. Smith, P. J., Hendricks, R. C., Steinetz, B. M., "Electrolytic co-deposition neutron production measured by bubble detectors", J. Electroanal. Chem., 882 (2021) 115024. https://doi.org/10.1016/j.jelechem.2021.115024
14. Oppenheimer, J. R., and Phillips, M., Phys. Rev. 48, 500 (1935).
15. Mosier-Boss, P.A., Forsley, L.P.G. and McDaniel, P., "Investigation of Nano-Nuclear Reactions in Condensed Matter: Final Report", *Defense Threat Reduction Agency*, (June 2016) pp 1-104. http://dx.doi.org/10.13140/RG.2.2.31859.53282
16. Forsley, L.P., "Space Power: The Genie Fast-Fission Sub-Critical Core", American Nuclear Society, Nuclear and Emerging Technologies for Space, NETS-2018 (Las Vegas, NV) (February 28, 2018).
17. Forsley, L.P., T.L. Benyo, P.A. Mosier-Boss, M.R. Deminico, L. A. Dudzinski, "Molten Salt Lattice Confinement Fusion (LCF) Fast Fission Reactor for Lunar and Planetary Surface Power", American Nuclear Society, Nuclear and Emerging Technologies for Space, NETS-2022 (Cleveland, NV) (May 11, 2022).
18. Gibson, M., et. al., "Heat Transport and Power Conversion of the Kilopower Reactor Test", Nuclear Technology, 206(31-42) (2020) 31-42.
19. DeChiaro, L. F., et al., "A Multi-Laboratory Study of Anomalous Elements and Magnetic Field Orientation Effects in LENR Codeposition Experiments", in review (2021).

20. US Patent 8,419,919, “System and Method for Generating Particles”
21. Liaw, B.Y., and Ding, T., “Charging Hydrogen into Ni in Hydride-containing Molten Salts”, Office of Naval Research, ONR Report # 04, Grant No. N00014-92-J-1673 (January, 1994)
22. Zimmerman, W., R. Bonitz and J. Feldman, "Cryobot: an ice penetrating robotic vehicle for Mars and Europa," 2001 IEEE Aerospace Conference Proceedings (Cat. No.01TH8542), Big Sky, MT, USA, 2001, pp. 1/311-1/323 vol.1, https://doi.org/10.1109/AERO.2001.931722
23. do Vale Pereira, P., et al., “Experimental validation of Cryobot thermal models for the exploration of ocean worlds”, The Planetary Science Journal, 4:81 (23pp), 2023 May. https://doi.org/10.3847/PSJ/acc2b7
24. Durka, M. J., et al., “A Novel High-Performance Mission-Enabling Multi-Purpose Radioisotope Heat Source”, 2022 IEEE Aerospace Conference, https://doi.org/10.1109/AERO53065.2022.9843667
25. Woerner, D., et al., “Radioisotope heat sources and power systems enabling ocean worlds subsurface and ocean access missions,” Bulletin of the American Astronomical Society, vol. 53, no. 4, p. 322, May 2021.
26. Dyson, R., “True Zero Emission Electric Aircraft Propulsion Transport Technology”, AIAA Aviation 2023 Forum, 12-16 June 2023, San Diego, CA. https://arc.aiaa.org/doi/10.2514/6.2023-3987
27. Mosier-Boss, P.A. Forsley, L.P., and McDaniel, P., “Uranium Fission Using Pd/D Co-deposition”, *JCMNS*, **29**, (2019), 219-229. https://doi.org/10.70923/001c.72504
28. Dyson, R., “Nuclear Electric Strayton Propulsion”, Energy & Mobility Technology, Systems and Value Chain Conference & Expo, Sept. 12-15, 2023, Cleveland, OH
29. Mason, L., “A Comparison of Brayton and Stirling Space Nuclear Power Systems for Power Levels from 1 Kilowatt to 10 Megawatts”, (January 1, 2000). https://ntrs.nasa.gov/citations/20010016863
30. Mason, L., “Recent Advances in Power Conversion and Heat Rejection Technology for Fission Surface Power”, *NASA/TM*—2010-216761, (2010). https://ntrs.nasa.gov/citations/20100029633
31. Forsley, L., “Detection of neutron activation in seawater”, GEC, (Feb 10, 2024).
32. https://peakeasy.lanl.gov
33. https://www.oecd-nea.org/jcms/pl_39910/janis
34. US Patent 12,092,054, “Combined Brayton and Stirling Cycle Power Generator”
35. Jain, A. *et al*., “Commentary: The Materials Project: A materials genome approach to accelerating materials innovation”, *APL Materials*, **1**, (2013) 011002. https://doi.org/10.1063/1.4812323
36. Ziegler, J. F., Ziegler, M.D. Biersack, J.P., “SRIM – The Stopping and range of ions in matter”, *Nuclear Inst. And Methods in Physics Research Section B: Beam Interactions with Materials and Atoms*, **268**(11-12) (June 2010) 1818-1823. https://doi.org/10.1016/j.nimb.2010.02.091
37. Truscello, V., “The Program at JPL to Investigate the Nuclear Interaction of RTFs with Scientific Instruments On Deep Space Probes”, *JPL,* (January 1, 1971) https://ntrs.nasa.gov/api/citations/19720010068/downloads/19720010068.pdf